

## INVERSION BASED TRAJECTORY TRACKING CONTROL FOR A PARALLEL KINEMATIC MANIPULATOR WITH FLEXIBLE LINKS

Markus T. Burkhardt\*, Philip S. Holzwarth, Robert Seifried

University of Stuttgart  
Institute of Engineering and Computational Mechanics  
Stuttgart, Germany  
{markus.burkhardt,philip.holzwarth,robert.seifried}@itm.uni-stuttgart.de

**Keywords:** FMBS, Trajectory Tracking, Feed-Forward, Model-Order Reduction, Spill-Over.

**Abstract.** *Trajectory tracking of flexible multibody systems is a challenging task since they possess more degrees of freedom than control inputs and impede the direct measurement of the assumed generalised coordinates. In this paper a control approach based on combined inversion-based feed-forward and feedback control is presented. The testing example used is a parallel manipulator with highly flexible arms. The assembly consists of a long and a short arm each mounted on a car. The end of the short arm is connected to the middle of the long arm with a revolute joint. The elastic arms are modelled as Timoshenko beams using the finite element method which are connected with rigid bodies and undergo a model-order reduction. These numerically efficient models are incorporated in the multibody system using the floating frame of reference approach. The end-effector of the long arm is supposed to follow a predefined trajectory.*

*In this paper we are going to present an appealing way to incorporate the kinematic loop as well as the feed-forward control problem into the modelling of flexible multibody systems. The arising differential-algebraic equations contain the remaining dynamics of the system under the presence of the constraints and give the inverse model. Due to the inclusion of the feed-forward control, the inverse model is unstable and has to be solved as a boundary value problem.*

*Based on these results a control approach that consists of the pre-computed feed-forward control and an output controller that incorporates solely the car positions, the joint angles and the arm curvature obtained by strain gauges is presented. This combination promises high-accuracy position tracking with a low on-line computational effort. The set-up is tested on various models which differ in the dimension of the reduced elastic bodies and in the used reduction techniques. It is shown that, depending on the chosen reduction method, spill-over effects can be minimised with a surprising small number of shape functions.*

## 1 Introduction

Structural vibrations impede the modelling as well as the control design of mechanical systems in many different respects. On the one hand, the modelling of such systems requires a strict trade-off between accuracy and efficiency more than other systems do. In other words, a suitable model needs to reflect these vibrations accurately whilst being small enough for control purposes. One commonly used approach to model such systems are flexible multibody systems. This formulation incorporates the flexibility of the system into the well-known framework for rigid body dynamics. With this approach, large non-linear working motions as well as small, elastic deformations can be described in a very efficient way. In this paper, the floating frame of reference approach is used to include the flexible bodies into the multibody system.

On the other hand, systems with significant deformations complicate the control design because there are more generalized coordinates than control inputs. In case of non-collocated inputs and outputs, these under-actuated systems might be non-minimum phase, which renders many control techniques impossible to apply. In addition, due to the large number of degrees of freedom, the reconstruction of all generalised coordinates might be impossible in practice.

In this paper, the modelling and control design of a parallel manipulator with flexible links, as seen in Figure 1, is presented. The end-effector of the long arm is supposed to follow a straight line in the horizontal plane. Starting with the meshing of the elastic parts and the downstream model order reduction, the assembly of the open-loop flexible multibody system using the floating frame of reference approach is performed in Neweul-M<sup>2</sup> [1]. Afterwards, geometrical constraints are imposed to close the kinematic loop between the two arms. The present set of differential-algebraic equations is transformed to a set of ordinary differential equations.

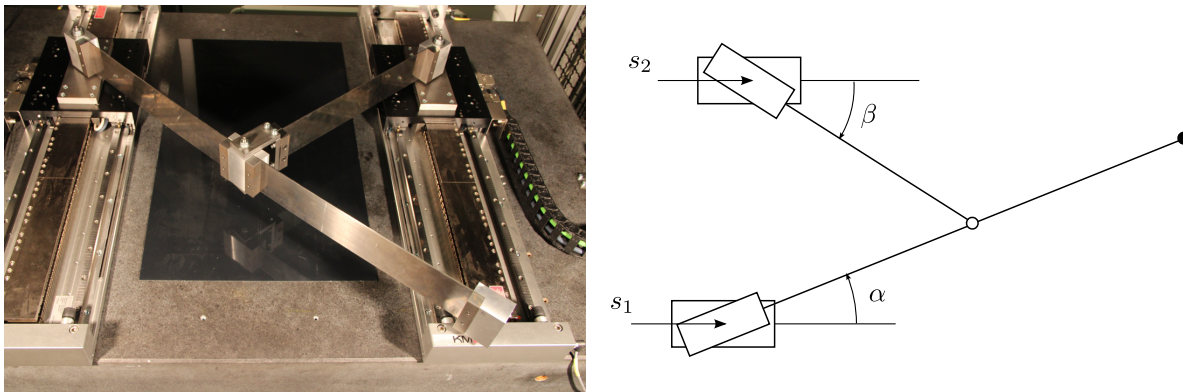


Figure 1: Test stand of a parallel manipulator with flexible links to the left and a schematic sketch to the right.

A two degrees of freedom control approach is used to achieve end-effector trajectory tracking of the parallel manipulator. At first, the feed-forward control, which allocates the set values of the control inputs as well as of all generalised coordinates and their derivatives, is computed offline. The feed-forward control is obtained by exact model inversion [2, 3] which requires in case of end-effector trajectory tracking the solution of a two-point boundary value problem. Based on the pre-computed set values, simple feedback controllers are used to compensate small model uncertainties and disturbances.

## 2 Model Set-up

The chosen two degrees of freedom control approach demands high accuracy models to achieve end-effector trajectory tracking. The modelling process can be separated into two major parts. At first, the flexible components of the system are modelled with the finite element method. Then, the flexible multibody system is assembled in the research code *Neweul-M<sup>2</sup>*.

### 2.1 Pre-Processing

The usage of the floating frame of reference approach requires various pre-processing steps. At first, the flexible parts, i.e. the thin parts of the long link shown in Fig. 2, are modelled using Timoshenko beam elements. For each segment, one hundred beam elements, which are constrained to the horizontal plane, are used. But instead of creating two separated bodies, both segments are combined in one elastic body. In addition, the rigid bodies, which are located at the joints and the end-effector, are attached to the flexible segments. Therefore, the defined elastic bodies consists of three rigid bodies and two hundred beam elements and accordingly, six hundred degrees of freedom. With this approach, a realistic definition of the boundary conditions is possible. For the incorporation in the flexible multibody system a reference frame must be defined. Therefore, the two translations of the nodal frame at the first joint as well as one translation of the nodal frame located at the second joint, which connects the two links, are locked. This kind of boundary condition is very similar to the chord frame definition and, here, the natural choice for the considered system.

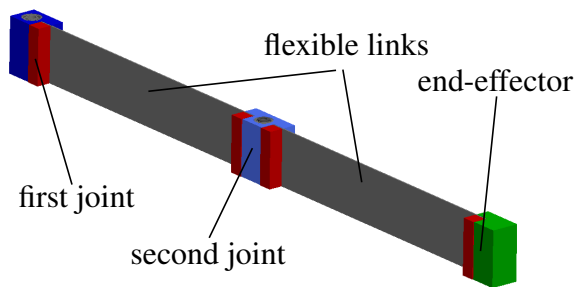


Figure 2: Long link of the parallel manipulator.

In a next step, a model order reduction of the elastic body is performed in order to efficiently incorporate the flexible arm in a multibody system. Next to the classical approach of modal truncation, some modern reduction techniques are used to condensate the model for control purposes. In contrast to modal truncation, these methods reduce the system dimension with respect to the transfer function or the Gramian matrices of the system. Therefore, these methods require the definition of system inputs and outputs. For mechanical systems it is reasonable to stick to collocated inputs and outputs. This restriction conserves important properties of mechanical systems, e.g. stability and passivity. Therefore, it is assumed that the output matrix  $C_e$  equals the transposed input matrix  $B_e$ .

The system description needed for these reduction techniques can be stated as a set of linear differential equations in the elastic coordinates  $q_e$  according to

$$M_{ee} \cdot \ddot{q}_e + D_{ee} \cdot \dot{q}_e + K_{ee} \cdot q_e = B_e \cdot u_e, \quad (1a)$$

$$y_e = C_e \cdot q_e. \quad (1b)$$

Here, the mass matrix  $M_{ee}$ , the damping matrix  $D_{ee}$  and the stiffness matrix  $K_{ee}$  determine the system dynamics. The system inputs  $u_e$  act on the dynamics via the input matrix  $B_e$ . The output matrix  $C_e$  maps the elastic coordinates  $q_e$  to the outputs  $y_e$ .

The first modern approach is called moment matching and is based on Krylov subspaces. This method matches the transfer function of the elastic bodies at certain frequencies up to a defined order. The second modern reduction method is based on frequency-weighted balanced truncation. This method utilises the Gramian matrices of the system to obtain the reduced basis by means of the energy related to the actuation and observation of the states, respectively. The method which was used here approximates these Gramian matrices with a Proper Orthogonal Decomposition (POD). A more detailed presentation of these methods can be found in [4].

The last method is a modification of the Craig-Bampton method [5]. This hybrid method, presented for the first time in [6], combines the advantages of the well-proved Craig-Bampton scheme and a powerful Gramian-based approach. Constraint modes are used to ensure that the reduced system can handle time-varying boundary conditions at defined interaction degrees of freedom. The difference to the traditional Craig-Bampton scheme is the treatment of the remaining inner dynamics. Instead of eigenmodes, in the new approach shape functions arising from a Gramian-based reduction are applied. The inner dynamics are excited by acceleration of the constraint modes, and thus inertia forces are taken as inputs for the calculation of the Gramians.

For the Krylov and POD methods, the inputs acting on the elastic structure result from the rigid body motion initiated by the cars of the linear motors. Therefore, it is necessary to revise the Newton-Euler equations of a free elastic body in the floating frame of reference approach. Next to the dynamics of the elastic structure stated in Eq. (1a), the rigid body dynamics have to be considered. The equations of motion of the isolated body can be stated as

$$\overline{M} \cdot z + h_\omega + h_e = h_g + \sum_{i=1}^k T_{T,i} \cdot F_i + T_{R,i} \cdot L_i. \quad (2)$$

The vector  $z$  summarises the accelerations  $a$ , the angular accelerations  $\alpha$  of the reference frame and the elastic accelerations  $\ddot{q}_e$ . Within this notation  $h_\omega$  comprises the Coriolis, centrifugal and Euler forces, which depend on the chosen reference frame. The term  $h_e$  consists of the elastic forces, which are defined by the stiffness and damping matrices. The terms on the right-hand side of the equation describe imposed forces or moments acting on the bodies as well as the force of inertia  $h_g$  caused by the gravity. In this context, the matrices  $T_{T,i}$  and  $T_{R,i}$  map the forces  $F_i$  and moments  $L_{j,i}$  acting on the nodal frame  $i$  to the reference frame of the body  $j$ . The  $(6 + n_{\text{elast}}) \times (6 + n_{\text{elast}})$  mass matrix  $\overline{M}$ , which might be dense for some reference frames, can be stated as

$$\overline{M} = \begin{bmatrix} M_{tt} & M_{tr} & M_{te} \\ M_{rt} & M_{rr} & M_{re} \\ M_{et} & M_{er} & M_{ee} \end{bmatrix}. \quad (3)$$

The indices of the submatrices t, r and e refer to translational, rotational and elastic.

Under the assumption, that the elastic deformations are small and in a neighbourhood of the static equilibrium, the vector  $h_\omega$  can be neglected. In addition, the vector  $h_g$  vanishes, because the elastic body is constrained to the horizontal plane, which is orthogonal to the gravitational acceleration vector  $g$ . Finally, by treating the existing, dominant components of the rigid body accelerations as the system inputs, Eq. (2) simplifies to

$$M_{ee} \cdot \ddot{q}_e + D_{eee} \cdot \dot{q}_e + K_{ee} \cdot q_e = -a_y M_{et,y} - \alpha_z M_{er,z}. \quad (4)$$

Thereby,  $a_y$  and  $a_z$  are the accelerations of the reference frame of the body. Then, the aggregation of the matrices  $M_{\text{et},y}$  and  $M_{\text{er},z}$  corresponds to the input matrix  $B_e$ .

The presented methods are used to create reduced elastic bodies of different dimensions. Afterwards, the reduced elastic bodies are exported to the SID-file format [7]. Subsequent to the assembly of the flexible multibody system, a convergence analysis and comparison of the presented methods is performed.

## 2.2 Flexible Multibody System

The flexible multibody system is assembled in the research code *Neweul-M<sup>2</sup>*. Next to the elastic body representing the long arm, three additional bodies have to be considered. These are the short arm, which is supposed to be rigid, and the two cars of the linear motors. In addition, the forces of the linear motors, which are modelled as the product of a motor constant and the motor current, and viscous dampers have to be included. For the statement of the Newton-Euler equations of the four bodies, the joint which connects the two arms, is cut open. Next to the reduced elastic coordinates  $\mathbf{q}_{\text{red}}$  four additional generalised coordinates are needed to describe the kinematics of the open-loop system, see Fig. 1. These are the car positions  $s_1$  and  $s_2$  as well as the joint angles  $\alpha$  and  $\beta$  of the arms. The application of D'Alembert's principle yields the equations of motion of the open-loop system. In order to close the loop, two kinematic constraints are defined. The arising set of differential-algebraic equations can be stated as

$$M(\mathbf{q}) \cdot \ddot{\mathbf{q}} = \mathbf{f}(\mathbf{q}, \dot{\mathbf{q}}) + \mathbf{B} \cdot \mathbf{u} + \mathbf{C}^T(\mathbf{q}) \cdot \boldsymbol{\lambda}, \quad (5a)$$

$$\mathbf{0} = \mathbf{c}(\mathbf{q}). \quad (5b)$$

The generalised mass matrix  $M$  is symmetric, positive definite and depends on the joint angles and the elastic coordinates. The generalised force vector  $\mathbf{f}$  summarises the generalised centrifugal, Coriolis, Euler and applied forces, except the forces, which are introduced by the system inputs  $\mathbf{u}$  together with the input matrix  $\mathbf{B}$ . The matrix  $\mathbf{C}$  is the Jacobian matrix of the constraint equations  $\mathbf{c}$  with respect to the generalised coordinates  $\mathbf{q}$ .

For the controller synthesis, the set of differential-algebraic equations is turned into a set of ordinary differential equations by a coordinate partitioning approach [8]. At first, the constraint equations are differentiated twice with respect to the time  $t$  yielding

$$\mathbf{0} = \ddot{\mathbf{c}} = \mathbf{C} \cdot \ddot{\mathbf{q}} + \frac{\partial(\mathbf{C} \cdot \dot{\mathbf{q}})}{\partial \mathbf{q}} \cdot \dot{\mathbf{q}}, \quad (6)$$

in which the second term is hereinafter referred to as  $\mathbf{c}''$ . In the next step, the vector of the generalised accelerations is separated into dependent accelerations  $\ddot{\mathbf{q}}_{\text{dep}}$  and independent accelerations  $\ddot{\mathbf{q}}_{\text{ind}}$ , which results in  $\mathbf{0} = \mathbf{C}_{\text{dep}} \cdot \ddot{\mathbf{q}}_{\text{dep}} + \mathbf{C}_{\text{ind}} \cdot \ddot{\mathbf{q}}_{\text{ind}} + \mathbf{c}''$ . This allows the restatement of the generalised accelerations in terms of the independent accelerations according to

$$\ddot{\mathbf{q}} = \begin{bmatrix} \mathbf{I} \\ -\mathbf{C}_{\text{dep}}^{-1} \cdot \mathbf{C}_{\text{ind}} \end{bmatrix} \cdot \ddot{\mathbf{q}}_{\text{ind}} + \begin{bmatrix} \mathbf{0} \\ -\mathbf{C}_{\text{dep}}^{-1} \cdot \mathbf{c}'' \end{bmatrix} = \mathbf{J}_C \cdot \ddot{\mathbf{q}}_{\text{ind}} + \boldsymbol{\gamma}. \quad (7)$$

Finally, the generalised accelerations in Eq. (5a) are substituted with Eq. (7) and the arising equations are multiplied with the transposed Jacobian matrix  $\mathbf{J}_C$  from the left yielding

$$\mathbf{J}_C^T \cdot M(\mathbf{q}) \cdot \mathbf{J}_C \cdot \ddot{\mathbf{q}}_{\text{ind}} = \mathbf{J}_C^T \cdot (\mathbf{f}(\mathbf{q}, \dot{\mathbf{q}}) - M(\mathbf{q}) \cdot \boldsymbol{\gamma}) + \mathbf{J}_C^T \cdot \mathbf{B} \cdot \mathbf{u}, \quad (8)$$

$$M_{\text{ind}}(\mathbf{q}) \cdot \ddot{\mathbf{q}}_{\text{ind}} = \mathbf{f}_{\text{ind}}(\mathbf{q}, \dot{\mathbf{q}}) + \mathbf{B}_{\text{ind}} \cdot \mathbf{u}. \quad (9)$$

For initial value problems, it is feasible to transform these equations back to the generalised coordinates according to  $\ddot{\mathbf{q}} = \mathbf{J}_C \cdot \mathbf{M}_{\text{ind}}(\mathbf{q})^{-1} (\mathbf{f}_{\text{ind}}(\mathbf{q}, \dot{\mathbf{q}}) + \mathbf{B}_{\text{ind}} \cdot \mathbf{u}) + \boldsymbol{\gamma}$ . These projected equations of motion do not depend on the Lagrange multipliers  $\boldsymbol{\lambda}$  and can be solved with standard ODE solvers.

### 2.3 Convergence analysis

In order to judge the different model reduction methods, a benchmark test has been performed. The models differ in the reduction techniques as well as in the number of shape functions used to describe the elastic body. The testing scenario is created by a movement of the cars under realistic velocity and acceleration profiles. The quality of the reduced models is determined by the error of the end-effector position and the curvature measured at a node of the second arm segment near the second joint, see Fig. 2. The reference solution is obtained by a simulation of a flexible multibody model, in which the full elastic body has not been reduced, i.e. with 600 elastic degrees of freedom.

Figure 3 shows the maximum absolute error of the end-effector position and the curvature. All presented methods show a fast convergence, but the new method CMSG based on the classical CMS approach together with Gramian-based reduction is by far the best, especially with respect to the curvature.

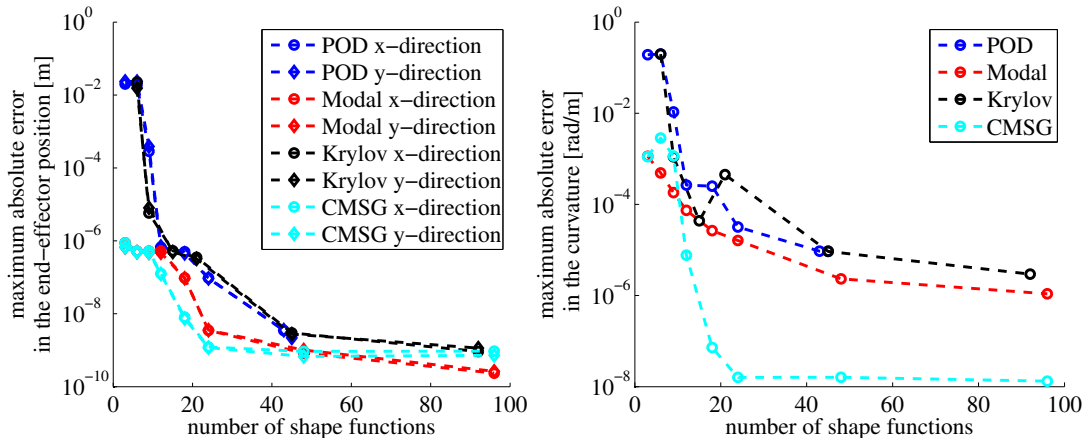


Figure 3: Comparison of the four different model order reduction methods: balanced truncation (POD), modal truncation (Modal), moment matching (Krylov) and the modified CMS (CMSG).

## 3 Control Concept

The control concept for end-effector trajectory tracking of the parallel manipulator is composed of two parts. At first, a feed-forward control by exact model inversion is computed. Then, based on the obtained set values, simple output controllers, which compensate small model uncertainties and disturbances, are set up.

### 3.1 Feed-forward control design

The feed-forward control is obtained by exact model inversion of the complete dynamical model. In a first step, the obtained equations of motions derived in Section 2 are augmented by additional constraint equations, the so-called servo constraints  $\mathbf{s}$ , [9, 10], to enforce trajectory

tracking. This yields the set of differential-algebraic equations

$$M(\mathbf{q}) \cdot \ddot{\mathbf{q}} = \mathbf{f}(\mathbf{q}, \dot{\mathbf{q}}) + \mathbf{B} \cdot \mathbf{u} + \mathbf{C}^T(\mathbf{q}) \cdot \boldsymbol{\lambda} \quad (10a)$$

$$\mathbf{0} = \mathbf{c}(\mathbf{q}) \quad (10b)$$

$$\mathbf{0} = \mathbf{s}(t, \mathbf{q}) \quad (10c)$$

This set of differential-algebraic equations describes the inverse model, which might be purely algebraic or contain a dynamical part. The dynamic part is called internal dynamics, which can not be influenced by the inputs  $\mathbf{u}$  and can not be observed in the servo constraints  $\mathbf{s}$ . In case of end-effector trajectory tracking, the internal dynamics of this flexible system is unstable, i.e. the system is non-minimum phase. This phenomenon is well-known for non-collocated input-output combinations. In such a case stable inversion [12] might be used. Thereby, it is necessary to solve a two-point boundary value problem, which results in bounded set values for the system inputs as well as for the generalised coordinates and their time derivatives.

The statement of the two-point boundary value problem suggests the transformation of the set of differential-algebraic equations in Eq. (10) to its embedded set of ordinary differential equations. This formulation is similar to Section 2.2, except that an oblique transformation of the constrained equations of motions is necessary. Here, it seems natural to use the elastic coordinates and their time derivatives as the reduced basis.

The solution of the boundary value problem is obtained with the Matlab solver `bvp5c`. The boundary conditions are stated in such way, that the solution starts on the unstable manifold and ends on the stable manifold of the internal dynamics. The obtained solution contains the set values of the minimal coordinates and their time derivatives. The set values of the dependent coordinates as well as the system inputs and Lagrange multipliers are computed from the constraint equations on position, velocity on acceleration level. These pre-computed computed generalised coordinates and system inputs will be referred to as  $\mathbf{q}_d$  and  $\mathbf{u}_{ff}$ , respectively.

### 3.2 Feedback controller

The feedback control concept incorporates cascade controllers for each car positions and an additional curvature controller [11], which is supposed to damp high-frequent oscillations of the elastic body. The latter controller uses a least-squares approach to merge the measurements of three strain gauges, which are applied on the long arm. Figure 4 shows the control structure, that is used for end-effector trajectory tracking. For simplicity, it is assumed that the dynamics of the mechanical system is dominant and the motor dynamics can be neglected. Otherwise, the cascade controllers could include an additional current loop.

In this presentation, the main focus lies on the design of the curvature controller. The reason why this approach is chosen, is based on the fact that is difficult to reconstruct the elastic coordinates from the strain gauge measurement in real-time, which would be necessary for a state feedback controller. However, it is very easy to obtain the signals of the strain gauges if the elastic coordinates are available.

Therefore, the first step is the computation of the desired curvature based on the offline computed desired values of the reduced elastic coordinates  $\mathbf{q}_{red}$ . The curvature  $\kappa$  of a Timoshenko beam is given by

$$\kappa(x) = \frac{\partial \psi_z(x)}{\partial x} \cdot \mathbf{q}_{red} , \quad (11)$$

in which the row vector  $\psi_z$  represents the shape function of rotation in z-direction. Due to the finite element approach, the values of the shape functions are only known at the nodes of the

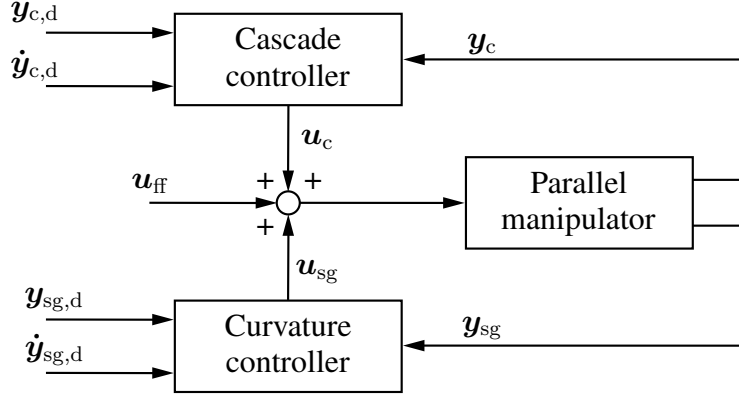


Figure 4: Control concept for end-effector trajectory tracking.

beam and the partial derivative can not be computed in a straight-forward way. Therefore, the actual shape function  $\psi_z(x)$  is approximated by cubic Hermite splines  $s(x)$ . The approximated curvature  $\kappa_{\text{approx}}$  is then obtained by

$$\kappa_{\text{approx}}(x) = \frac{\partial s(x)}{\partial x} \cdot \mathbf{q}_{\text{red}} = \mathbf{c}_\kappa(x) \cdot \mathbf{q} , \quad (12)$$

in which  $\mathbf{c}_\kappa(x)$  can be interpreted as a curvature shape function in terms of all generalised coordinates  $\mathbf{q}$ . The shape function  $\kappa_{\text{approx}}$  is now evaluated at the positions, where the strain gauges are applied. These discrete curvatures are now used to state the curvature output equation according to

$$\mathbf{y}_{\text{sg}} = \begin{bmatrix} \mathbf{c}_\kappa(x_1) \\ \vdots \\ \mathbf{c}_\kappa(x_p) \end{bmatrix} \cdot \mathbf{q} = \mathbf{C}_{\text{sg}} \cdot \mathbf{q} = \mathbf{C}_{\text{sg,ind}} \cdot \mathbf{q}_{\text{ind}} . \quad (13)$$

The first part of the curvature controller design is finding a suitable distribution matrix that connects the curvature errors  $\mathbf{e}_{\text{sg}} = \mathbf{y}_{\text{sg}} - \mathbf{y}_{\text{sg,d}}$  with the system inputs. Differentiating Eq. (13) twice with respect to the time and substituting the independent accelerations with Eq. (8) yields

$$\ddot{\mathbf{y}}_{\text{sg}} = \mathbf{C}_{\text{sg,ind}} \cdot \mathbf{M}_{\text{ind}}(\mathbf{q})^{-1} \cdot \mathbf{f}_{\text{ind}}(\mathbf{q}, \dot{\mathbf{q}}) + \mathbf{C}_{\text{sg,ind}} \cdot \mathbf{M}_{\text{ind}}(\mathbf{q})^{-1} \cdot \mathbf{B}_{\text{ind}} \cdot \mathbf{u} . \quad (14)$$

In the next step, a least-squares solution at a static equilibrium  $\mathbf{q} = \mathbf{q}_0$  is obtained via a QR-decomposition yielding

$$\mathbf{C}_{\text{sg,ind}} \cdot \mathbf{M}_{\text{ind}}(\mathbf{q}_0)^{-1} \cdot \mathbf{B}_{\text{ind}} = \mathbf{Q}_i \cdot \mathbf{R}_i . \quad (15)$$

Here, the matrix  $\mathbf{Q}_i$  spans the column space of the matrix product, which results in a square matrix  $\mathbf{R}_i$ . This representation is sometimes called economy-size QR-decomposition. In conjunction with the pre-computed input  $\mathbf{u}_{\text{ff}}$  and an additional input  $\mathbf{v}$ , Eq. (14) can be restated as

$$\ddot{\mathbf{y}}_{\text{sg}} = \mathbf{C}_{\text{sg,ind}} \cdot \mathbf{M}_{\text{ind}}^{-1} \cdot \mathbf{f}_{\text{ind}} + \mathbf{C}_{\text{sg,ind}} \cdot \mathbf{M}_{\text{ind}}^{-1} \cdot \mathbf{B}_{\text{ind}} \cdot (\mathbf{u}_{\text{ff}} + \mathbf{R}_i^{-1} \cdot \mathbf{Q}_i^T \cdot \mathbf{v}) , \quad (16)$$

$$\ddot{\mathbf{y}}_{\text{sg}} = \mathbf{C}_{\text{sg,ind}} \cdot \underbrace{\mathbf{M}_{\text{ind}}^{-1} \cdot (\mathbf{f}_{\text{ind}} + \mathbf{B}_{\text{ind}} \cdot \mathbf{u}_{\text{ff}})}_{\ddot{\mathbf{q}}_d} + \mathbf{C}_{\text{sg,ind}} \cdot \mathbf{M}_{\text{ind}}^{-1} \cdot \mathbf{B}_{\text{ind}} \cdot \mathbf{R}_i^{-1} \cdot \mathbf{Q}_i^T \cdot \mathbf{v} , \quad (17)$$



in which the product  $\mathbf{C}_{sg,ind} \cdot \ddot{\mathbf{q}}_d$  equals the second derivative of desired curvature  $\ddot{\mathbf{y}}_{sg,d}$ . In a neighbourhood of the static equilibrium  $\mathbf{q}_0$ , the error dynamics of the curvature output reduce to

$$\ddot{\mathbf{e}}_{sg} = \dot{\mathbf{y}}_{sg} - \dot{\mathbf{y}}_{sg,d} = \mathbf{Q}_i \cdot \mathbf{Q}_i^T \cdot \mathbf{v} , \quad (18)$$

Due to the fact that the matrix product  $\mathbf{Q}_i \cdot \mathbf{Q}_i^T$  is positive semi-definite, the control law for the new input  $\mathbf{v}$  is easy to design. With the diagonal, positive definite gain matrices  $\mathbf{G}_p$  and  $\mathbf{G}_d$ , the additional input can be stated as  $\mathbf{v} = -\mathbf{G}_p \cdot \mathbf{e}_{sg} - \mathbf{G}_d \cdot \dot{\mathbf{e}}_{sg}$ , and thus the error dynamics result in

$$\ddot{\mathbf{e}}_{sg} = -\mathbf{Q}_i \cdot \mathbf{Q}_i^T \cdot (\mathbf{G}_p \cdot \mathbf{e}_{sg} + \mathbf{G}_d \cdot \dot{\mathbf{e}}_{sg}) . \quad (19)$$

In case that the time derivatives of the curvature are not available, simple PID for the curvature outputs can be used.

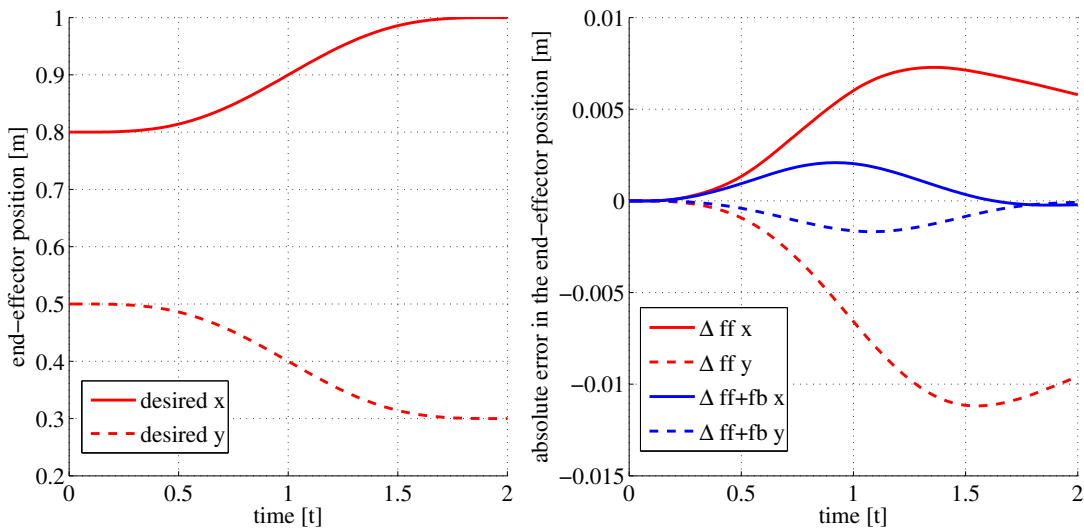


Figure 5: Comparison of the different model order methods.

In order to test the control, a feed-forward control based on a model twelve shape functions obtained by *CMSG* is computed. With the obtained set values, a simulation model with 96 eigenmodes is controlled with the presented controller structure. In addition, a mass of 200 g, which is not considered in the feed-forward control, is attached to the end-effector as a disturbance. Figure 5 shows the deviations of the end-effector position. In the presence of the additional mass, the maximum deviation of the end-effector is about 1.5 cm if no feedback is in use. This error drops to approx. 4 mm, if the controllers are active. In addition, the curvature controller does not cause spill-over effects, even though the simulation model included 96 shape functions.

#### 4 Conclusions

The modelling and control design for a parallel manipulator with flexible links has been presented. A very promising reduction method, which combines the advantages of the CMS approach and a Gramian-based reduction, has been introduced. This method promises small and accurate reduced models, which are used to design a feed-forward control that is supported by a cascade controller for the car positions and a output controller that incorporates the curvature of the flexible beams.

## Acknowledgment

The authors would like to thank the German Research Foundation (DFG) for financial support of the project within the Cluster of Excellence in Simulation Technology (EXC 310/1) at the University of Stuttgart and the project SE 1685/3-1.

## REFERENCES

- [1] T. Kurz, P. Eberhard, C. Henninger and W. Schiehlen, From Neweul to Neweul-M<sup>2</sup>: Symbolical Equations of Motion for Multibody System Analysis and Synthesis. *Multibody System Dynamics*, **24**, 25–41, 2010.
- [2] H. Zhao and D. Chen, Tip Trajectory Tracking for Multilink Flexible Manipulators using Stable Inversion. *Journal of Guidance, Control, and Dynamics*, **21**(2), 314–320, 1998.
- [3] R. Seifried, M. Burkhardt and A. Held, Trajectory Control of Serial and Parallel Flexible Manipulators using Model Inversion. J.C. Samin and P. Fisetts eds. *Multibody Dynamics: Computational Methods and Applications*, Computational Methods in Applied Sciences, Vol. 28, Springer, 2013.
- [4] C. Nowakowski, J. Fehr, M. Fischer and P. Eberhard, Model Order Reduction in Elastic Multibody Systems using the Floating Frame of Reference Formulation. *Full Paper Preprint Volume of MATHMOD Vienna - Vienna International Conference on Mathematical Modelling 2012*, Vienna, Austria, 2012.
- [5] W.C. Hurty, Dynamic Analysis of Structural Systems Using Component Modes. *AIAA Journal*, **3**, 678-685, 1965.
- [6] P. Holzwarth, Model Order Reduction for Coupled Bodies in Elastic Multibody Systems. *Poster at Model Reduction of Parametrized Systems MoRePaS II*, Günzburg, Germany, 2012.
- [7] O. Wallrapp, Standardization of Flexible Body Modeling in Multibody System Codes, Part I: Definition of Standard Input Data. *Mechanics of Structures and Machines*, **22**(3), 283-304, 1994.
- [8] G. Leister and D. Bestle. Symbolic-numerical Solution of Multibody Systems with Closed Loops. *Vehicle System Dynamics*, **21**(1), 129–142, 1992. 1996.
- [9] W. Blajer and K. Kolodziejczyk, A Geometric Approach to Solving Problems of Control Constrains: Theory and a DAE Framework. *Multibody System Dynamics*, **11**, 343-364, 2004.
- [10] R. Seifried and W. Blajer, Analysis of Servo-Constraint Problems for Underactuated Multibody Systems, *Mechanical Sciences, Special Issue: Recent Advances and Current Trends in Numerical Multibody Dynamics*, Vol. 4, 113-129, 2013.
- [11] H. Bremer and F. Pfeiffer, *Elastische Mehrkörpersysteme*. Teubner, Stuttgart, 1992.
- [12] S. Devasia, D. Chen and B. Paden, Nonlinear Inversion-Based Output Tracking. *IEEE Transactions on Automatic Control*, **41**(7), 930–942, 1996.